Supported $H_8PV_5Mo_7O_{40}$ on activated carbon: Synthesis and Investigation of influencing factors for catalytic performance

– Supporting information –

Anne Wesner[a#], Max P. Papajewski[a], Leon Schidowski[a], Charlotte Ruhmlieb[b], Maximilian J. Poller[a], Jakob Albert[a*]

[a] Institute of Technical and Macromolecular Chemistry, University of Hamburg, Bundesstraße 45, 20146 Hamburg, Germany

[b] Institute of Physical Chemistry, University of Hamburg, Grindelallee 117, 20146 Hamburg, Germany

* Contact details of the corresponding author: jakob.albert@uni-hamburg.de

Supplementary catalyst characterization

Analysis methods

ICP-OES inorganic elemental analysis

Elemental analysis of each catalyst was conducted using inductively coupled plasma optical emission spectrometry (ICP-OES). Each sample, weighing 100 mg, was dissolved in a solution of 5 mL aqua regia and 1 mL concentrated HF using the Anton Paar Multiwave 7000 microwave system. The sample was then atomized in an argon plasma, and its elemental composition was quantified through optical emission spectrometry. This analysis was carried out with an ASCOR spectrometer (by Spectro) at the central element analysis service of the Department of Chemistry, University of Hamburg

CHNS(O) organic elemental analysis

CHNS analysis was employed to determine the composition of activated carbon using the "Euro EA3000" instrument by EuroVector. The sample was encapsulated in a tin capsule and combusted in a helium stream with oxygen addition at approximately 1000°C (Euro EA). The resulting combustion gases were separated gas chromatographically and analyzed using a thermal conductivity detector (WLD), which compared the thermal conductivity of the gas mixtures to that of pure helium. This allowed the determination of the CHNS content with the aid of standard substances.

For determination of oxygen content, the "Oxycube" device from Elementar (-OC) was utilized. Here, the substance was weighed into a silver capsule and pyrolyzed at 1450°C on nickel-coated carbon powder in a helium stream. The resulting combustion gases were separated through absorption and desorption processes and analyzed with a thermal conductivity detector (WLD), comparing the thermal conductivity of the produced CO with that of pure helium. The oxygen content was then determined based on a calibration with standard substances. This characterization was carried out at the Central Element Analysis Service of the Department of Chemistry, University of Hamburg.

N_2-physisorption

The textural properties of the activated carbons were determined using N_2-physisorption measurements. These measurements were conducted with the SA3100 Surface Area Analyzer from Beckman Coulter. Prior to the analysis, samples were degassed under vacuum at 50 °C for 10 hours. This characterization was performed at the Interdisciplinary Centre for Analytics in the Nanoscale (ICAN Centre). Average pore diameter was measured by following equation:

$$\emptyset\ pore\ diameter\ (nm) = \sum_i pore\ diameter_i \cdot incremental\ volume_i$$

XRD

Crystal structure determination was performed through powder X-ray diffraction (p-XRD) using a Panalytical MDP X'Pert Pro diffractometer, operating in Bragg-Brentano geometry with Cu Kα radiation (λ = 0.1541 nm). The diffraction angle was measured over a range of 10 to 80°, with a sampling rate of 0.013° every 0.3 seconds.

NH_3-TPD

Acidity was assessed using NH_3-Temperature Programmed Desorption (NH_3 TPD) on a ChemBET Pulsar device from Quantachrome Instruments. Samples weighing 0.06 g were initially purged with helium gas (80 mL/min) and heated to 130 °C at a rate of 10 K/min for an hour to eliminate surface water. NH_3 adsorption on the surface was conducted at the same temperature. Subsequently, the samples were heated to 750 °C under a helium flow (80 mL/min, 10 °C/min), and the desorbed NH_3 was detected using a Thermal Conductivity Detector (TCD). The integration of the NH_3-TPD spectra areas, indicative of weak to medium (150-500 °C) and strong (500-700 °C) acidity, was performed with Origin software, normalizing all measurements to the CW20 standard.

Microscopy

Scanning electron microscopy (SEM) and energy-dispersive X-ray spectroscopy (EDX) revealed catalyst morphology and metal dispersion. All measurements, including images and maps, were conducted using the "Leo 1550 Gemini" system. For the imaging, an acceleration voltage of 2 kV and an aperture of 7.5 µm diameter were employed. Conversely, all mappings were performed with an acceleration voltage of 20 kV and a 30 µm aperture. The Silicon Drift Detector (SDD) "Ultim Max 100" from Oxford Instruments, in conjunction with the "AZtec" software, was utilized as the detector for these analyses.

Point of zero charge measurement

For the determination of the point of zero charge in 40 mL of sodium nitrate solution (0.1 M), the pH was adjusted using sodium hydroxide solution (0.1 M and 0.005 M) and nitric acid (0.1 M and 0.005 M). The pH was set to values ranging from 2 to 11 to create ten solutions with varying pH levels ($ph_{initial}$). These solutions were then treated with activated carbon (200 mg). The suspensions were stirred for 24 hours at 300 rpm on magnetic stirrer plates. Subsequently, the suspensions were filtered, and the pH of the filtrate was determined (pH_{final}).

To determine the point of zero charge (PZC), the ΔpH (pH_final - pH_initial) of each solution was calculated and plotted against the initial pH value of the solution. The linear region of the curve was fitted, and the intersection point, where ΔpH = 0) was determined as the PZC.

Boehm titration

Boehm titration method was used to determine the oxygen functional groups. Initially, the following solutions were prepared: NaOH (0.1 M), Na_2CO_3 (0.05 M), $NaHCO_3$ (0.1 M), and HCl (0.1 M). Activated carbon (2.00 g) was suspended in each of these solutions (50 mL). The four resulting suspensions were stirred for 24 hours. After stirring, the suspensions were filtered. To determine the amount of substance, 10 mL of each filtrate was titrated with either HCl or NaOH using an Eco Titrator of Metrohm.[1]

Infrared spectroscopy

Infrared spectroscopy was employed for structural elucidation. Infrared spectra were acquired using an attenuated total reflection (ATR) setup, specifically a QATR™-S single-reflection ATR system with a diamond prism, manufactured by Shimadzu. The raw spectral data were processed to correct the baseline, and peak identification was conducted manually. Subsequently, the IR spectral data were converted and exported as x/y text files for further analysis.

Raman spectroscopy

Raman spectroscopy was applied to elucidate the surface chemistry and structural features of the catalysts. Raman spectroscopic measurements were conducted using a SENTERRA Raman microscope by Bruker Optik GmbH. The instrument's aperture was adjusted to 50 x 1000 µm, and a 20x objective lens was employed. The excitation laser, operating at a wavelength of 785 nm, facilitated measurements in the range of 75 cm^{-1} to 1525 cm^{-1}. The parameters for these measurements included an integration time of 16 seconds, a total of 8 scans, and a laser power set to 10 mW.

Thermogravimetric analysis

Thermogravimetric analysis (TGA) was performed utilizing a NETZSCH TG 209 F1 Libra instrument. Data processing was carried out using the NETZSCH Proteus software. For each analysis, 20 mg of the sample was weighed into an Al2O3 crucible, and mass changes were recorded in accordance with the applied temperature program. The temperature protocol involved a ramp up to 200°C at a rate of 2 K/min, maintained for 3 hours, followed by cooling down to room temperature. Throughout the measurements, a nitrogen flow of 20 mL/min was continuously passed through the instrument.

Characterization of HPA-5

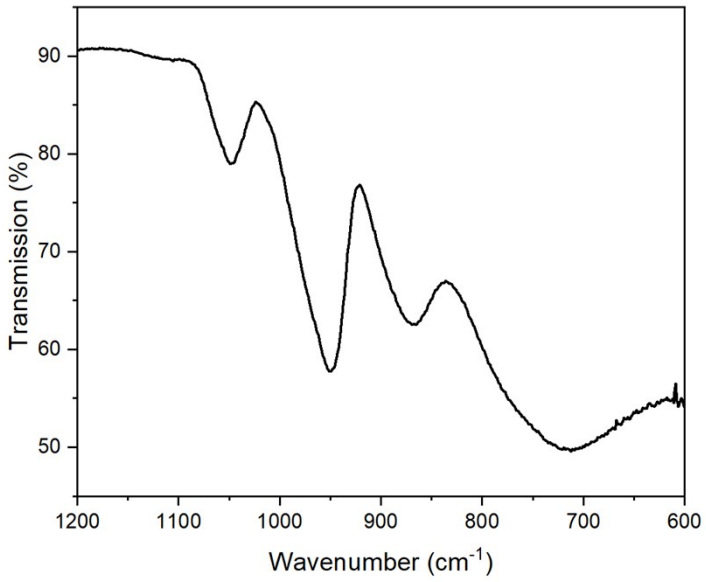

Figure S 1: Infrared spectra of bulk HPA-5.

Table S 1: Elemental and TGA analysis of bulk HPA-5.

	HPA-$5_{theor.}$	HPA-5
Loading[a]		
Mo (wt.%)[a]	41.84	36.19
P (wt.%)[a]	1.93	2.11
V (wt.%)[a]	15.87	13.86
Molar ratio Mo:V	7 : 5	7 : 5
Amount of Hydration water[b]		9.7 %

[a]determined via elemental analysis [b]determined via TGA analysis

Characterization of activated carbons

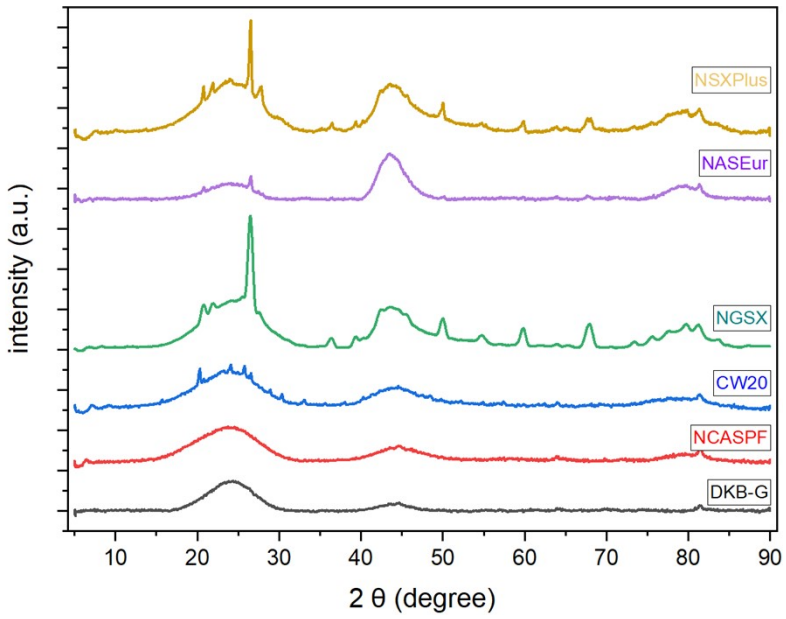

Figure S 2: XRD-diffractograms of pure activated carbons.

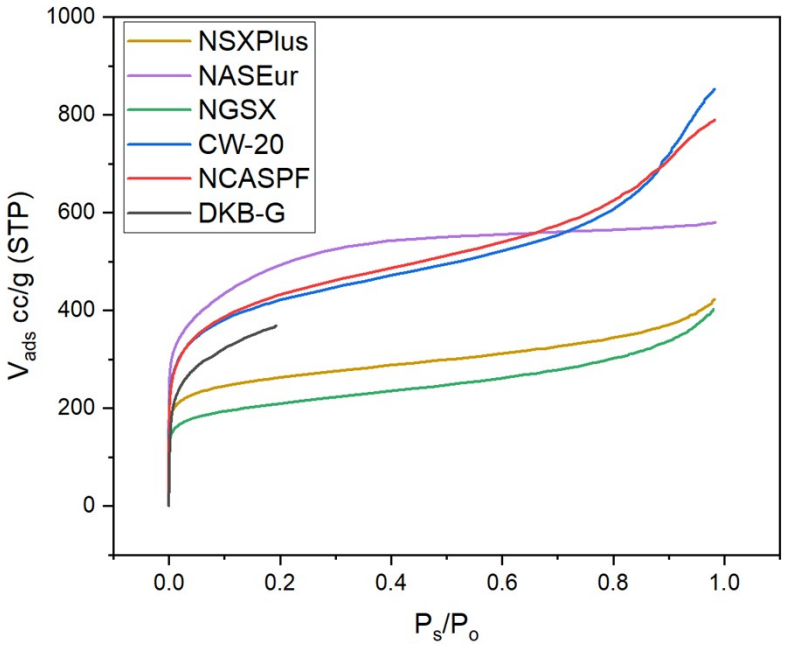

Figure S 3: Adsorption isotherms of pure activated carbons.

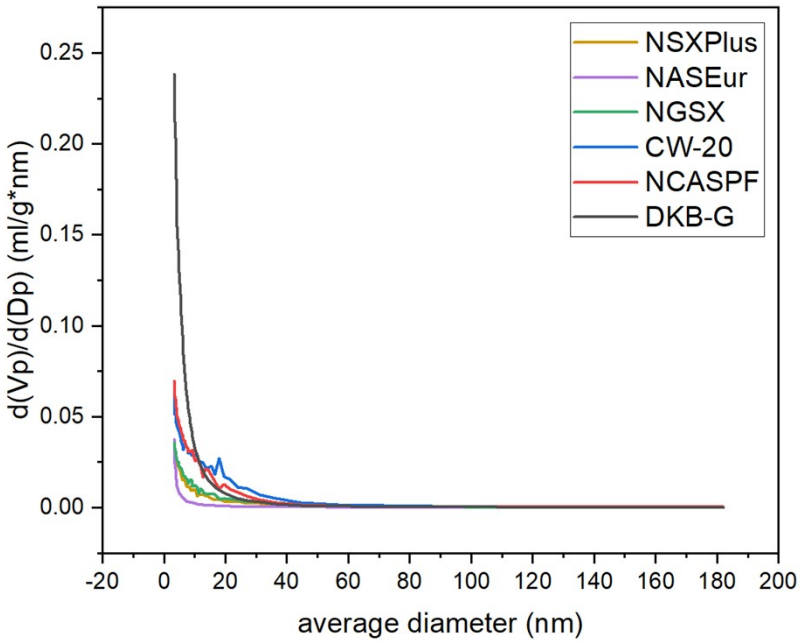

Figure S 4: Pore volumina of pure activated carbons.

Table S 2: Acidic properties of selected functional groups on carbon-based substrates.[2]

	Aqueous suspension
Carboxylic acid	Strong acidic
Anhdydrids	Strong acidic
Phenol	Acidic
Lactonic groups	Weakly acidic
Carbonyl groups	Weakly acidic
Pyrons	basic

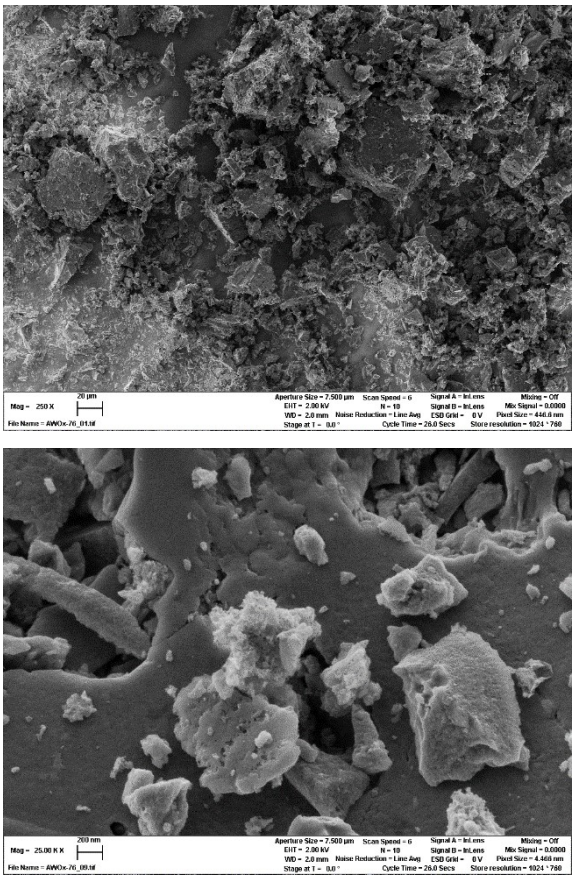

Figure S 5: SEM images of NSXPlus at magnifications of 250x and 25,000x.

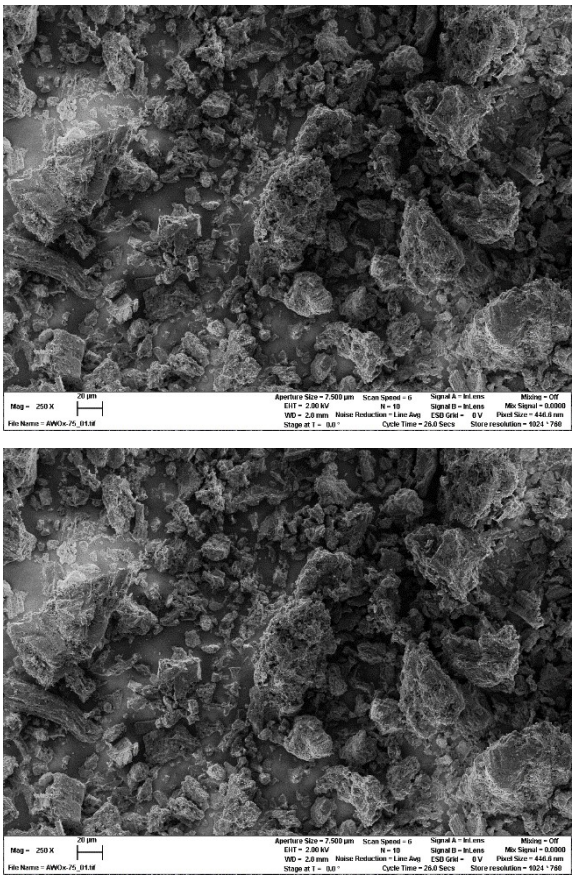

Figure S 6: SEM images of NASEur at magnifications of 250x and 25,000x.

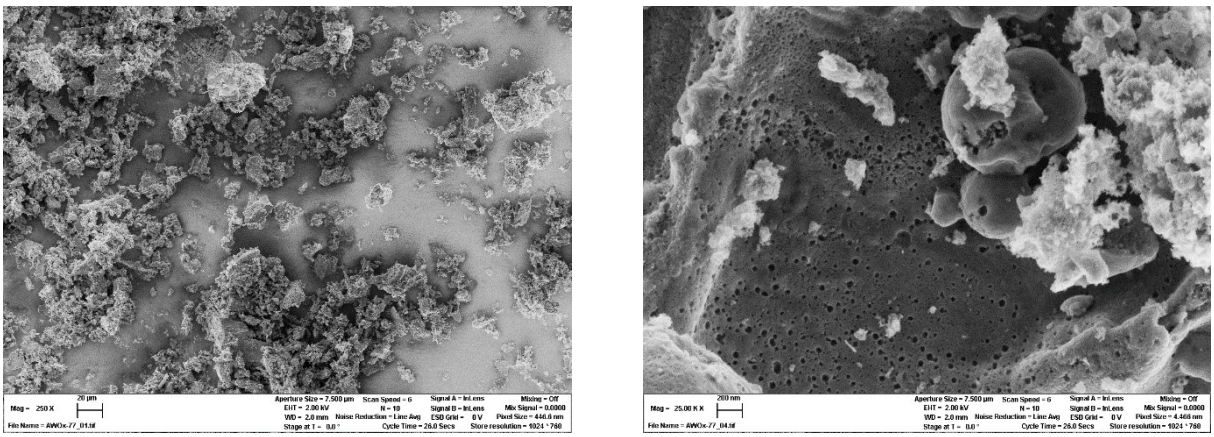

Figure S 7: SEM images of NGSX at magnifications of 250x and 25,000x.

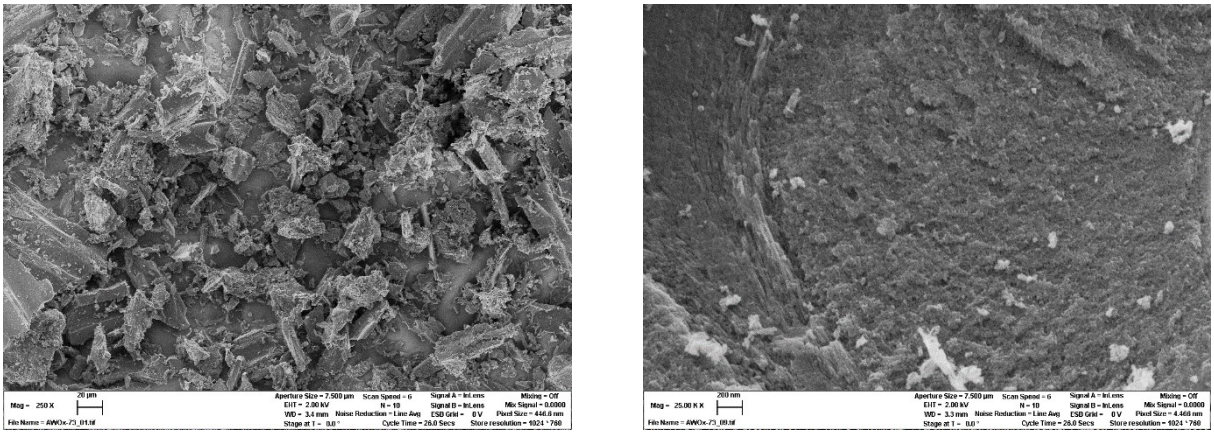

Figure S 8: SEM images of CW20 at magnifications of 250x and 25,000x.

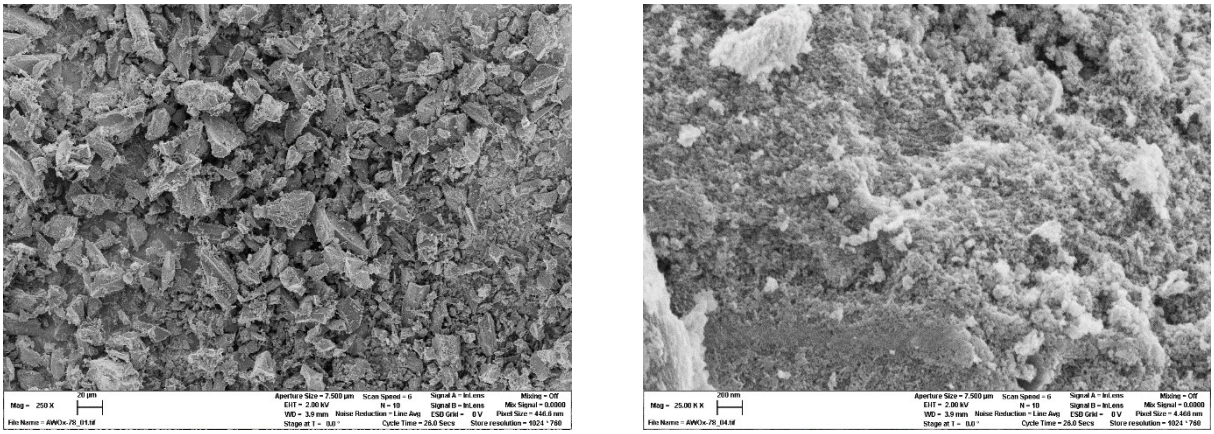

Figure S 9: SEM images of NCASPF at magnifications of 250x and 25,000x.

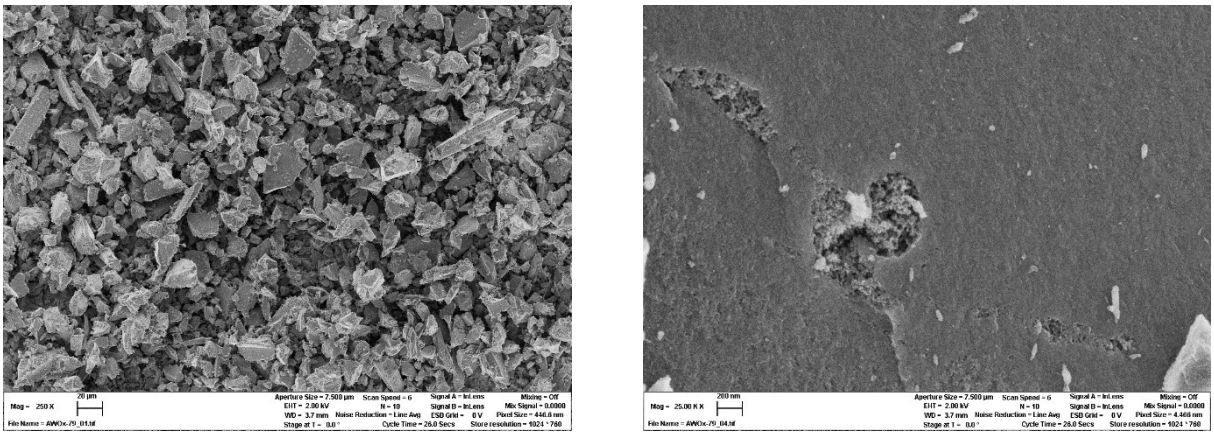

Figure S 10: SEM images of DKB-G at magnifications of 250x and 25,000x.

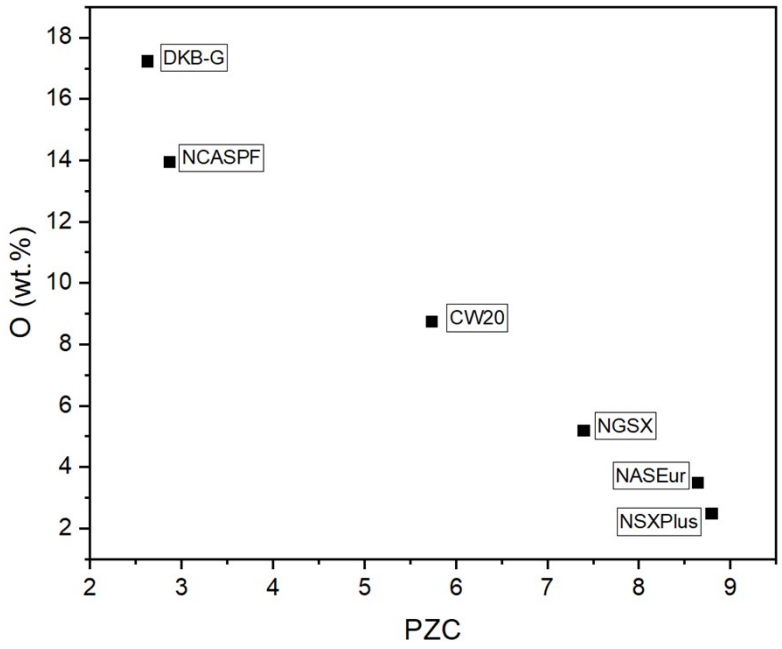

Figure S 11: Correlation between oxygen content and point of zero charge.

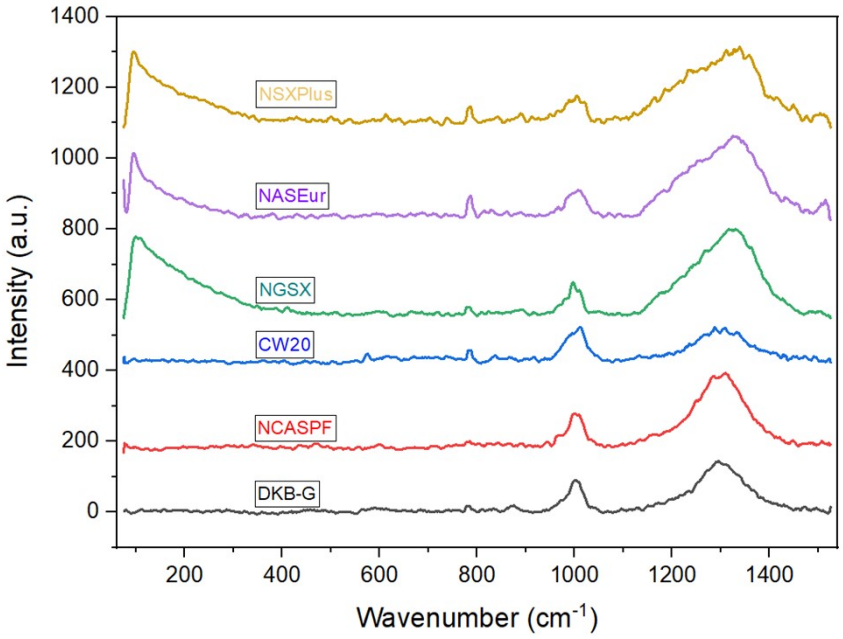

Figure S 12: Raman spectra of pure activated carbons.

Table S 3: positions of surface groups of activated carbons in infrared spectroscopy.[3]

	Assignment regions (cm-1)		
	1000-1500	1500-2050	2050-3700
C-O stretch of ethers	1000-1300		
Alcohols	1049-1276		3200-3640
Phenolic C-OH stretch	1000-1220		
Phenolic O-H bend/stretch	1160-1200		2500-3620
Carbonates	1100-1500	1590-1600	
Aromatics C=C stretching		1585-1600	
Quinones		1550-1680	
Carboxylic Acids (COOH)	1120-1200	1665-1760	2500-3300
Lactones	1160-1370	1675-1790	
Anhydrides	980-1300	1740-1880	
Ketones (C=C=O)			2080-2200
C-H stretch			2600-3000

HPA-5 supported on activated carbons

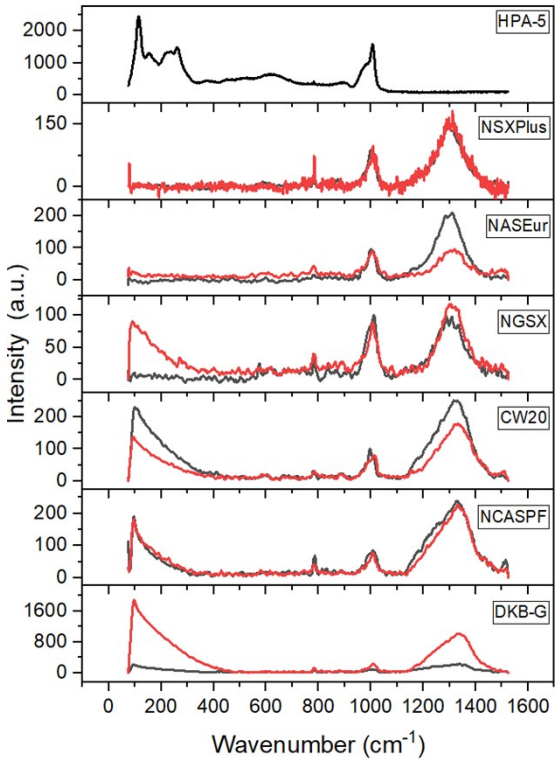

Figure S 13: Raman spectra of HPA-5 supported on various carbon materials.

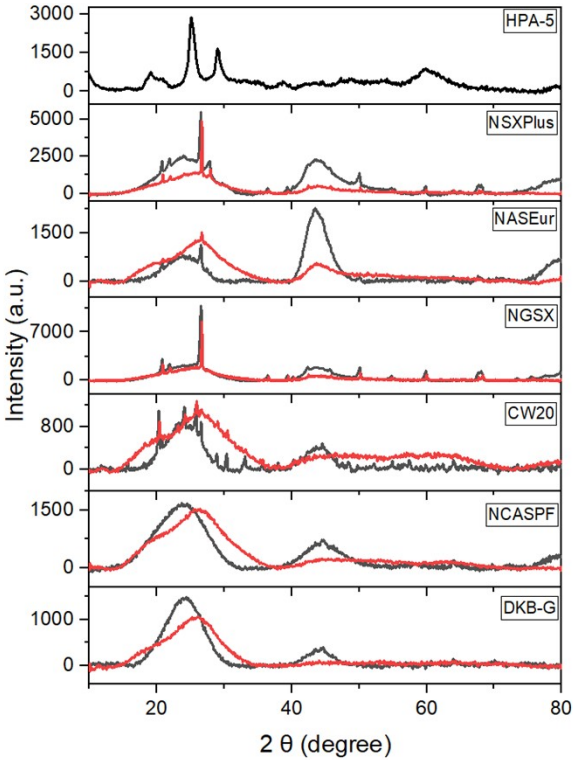

Figure S 14: XRD diffractograms of HPA-5 supported on various carbon materials.

NSXPlus

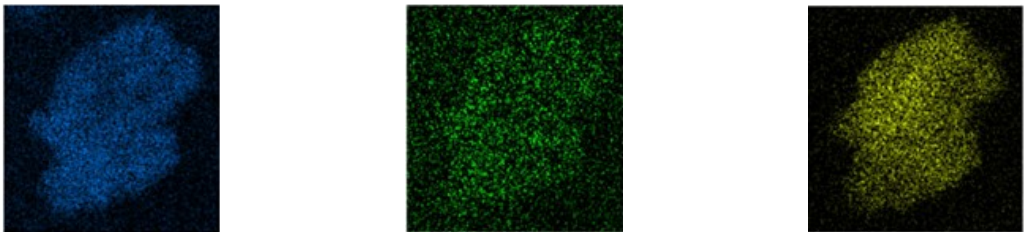

NASEur

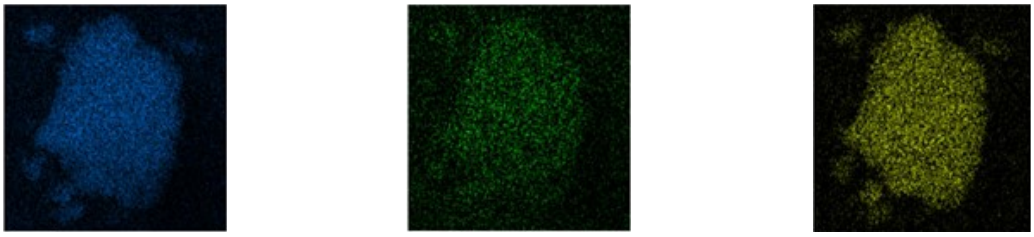

NGSX

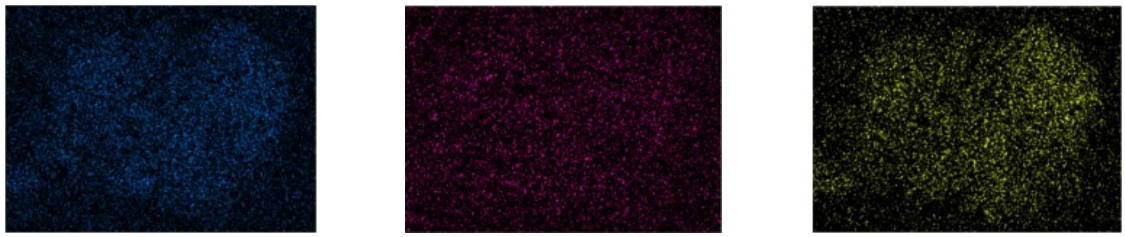

CW20

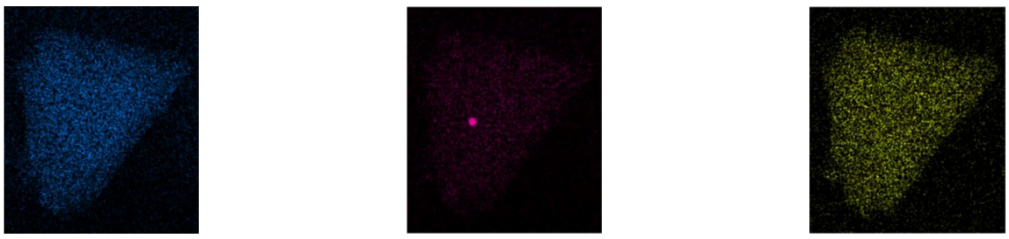

NCASPF

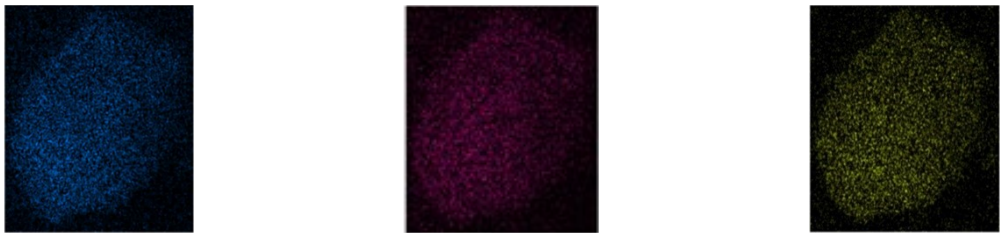

DKB-G

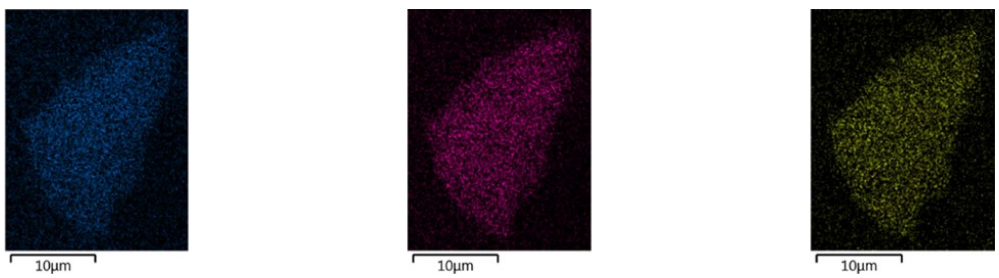

Figure S 15: SEM-EDX Mapping of impregnated carbons with Mo (blue), P (green & pink) and V (yellow).

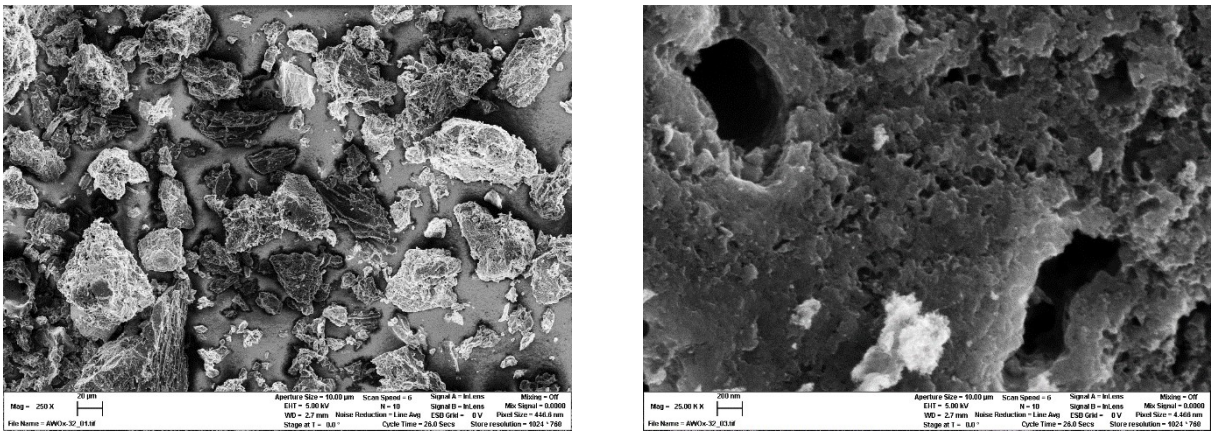

Figure S 16: SEM images of impregnated NSXPlus at magnifications of 250x and 25,000x.

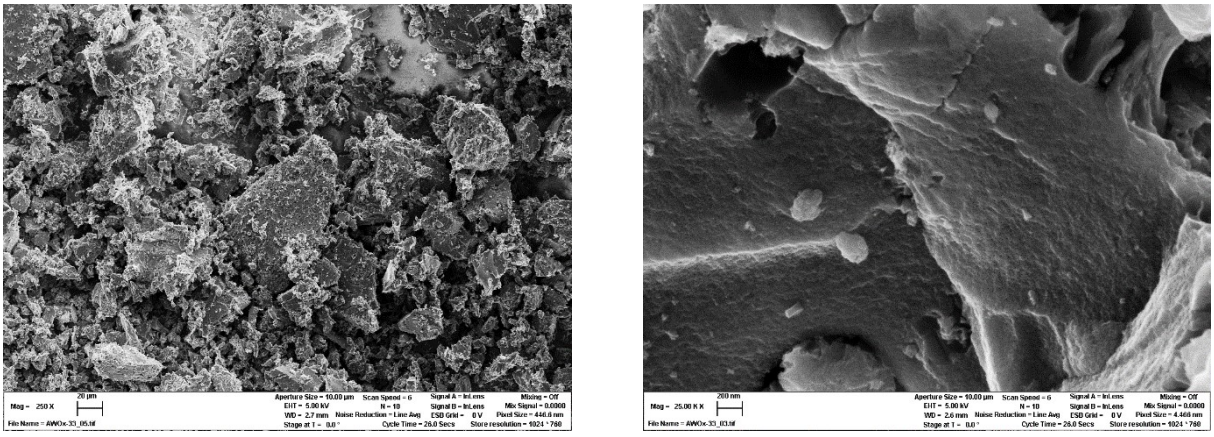

Figure S 17: SEM images of impregnated NASEur at magnifications of 250x and 25,000x.

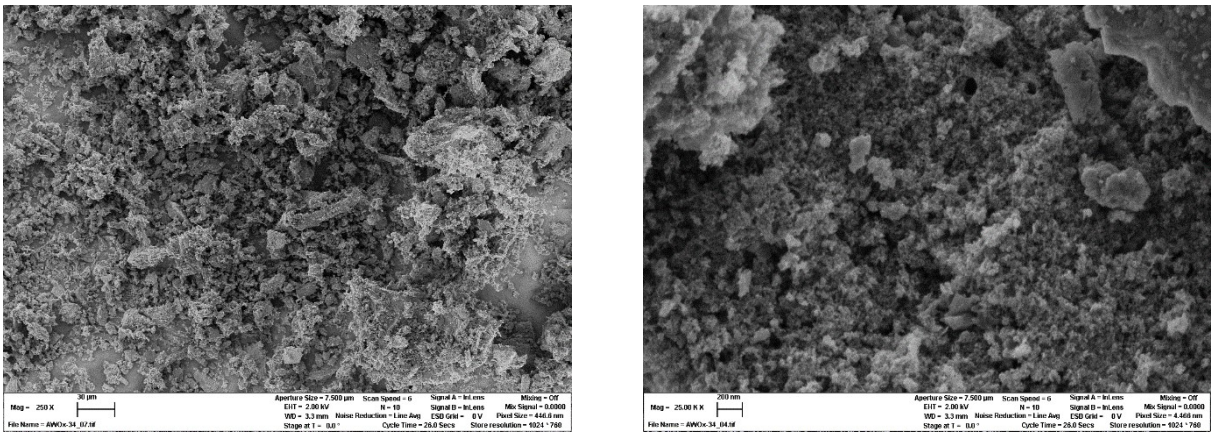

Figure S 18: SEM images of impregnated NGSX at magnifications of 250x and 25,000x.

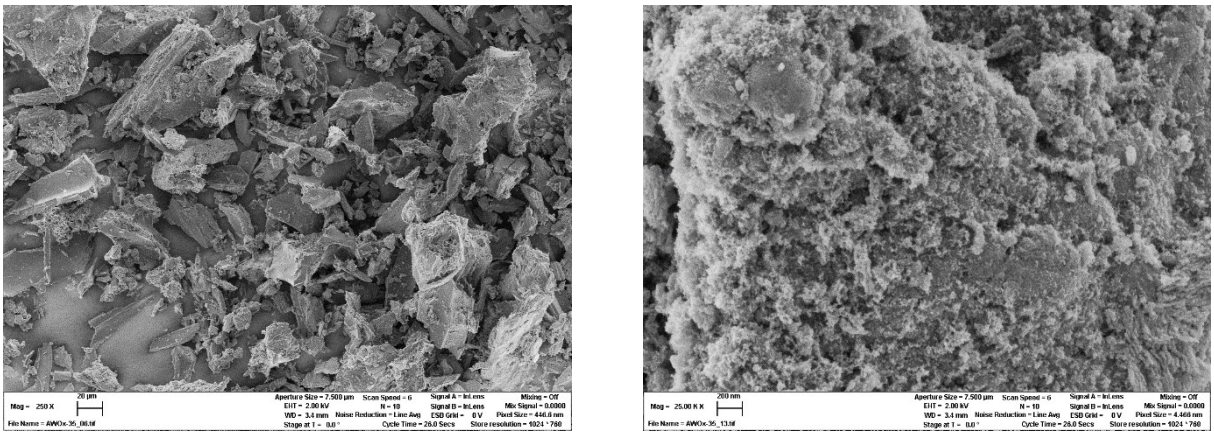

Figure S 19: SEM images of impregnated CW20 at magnifications of 250x and 25,000x.

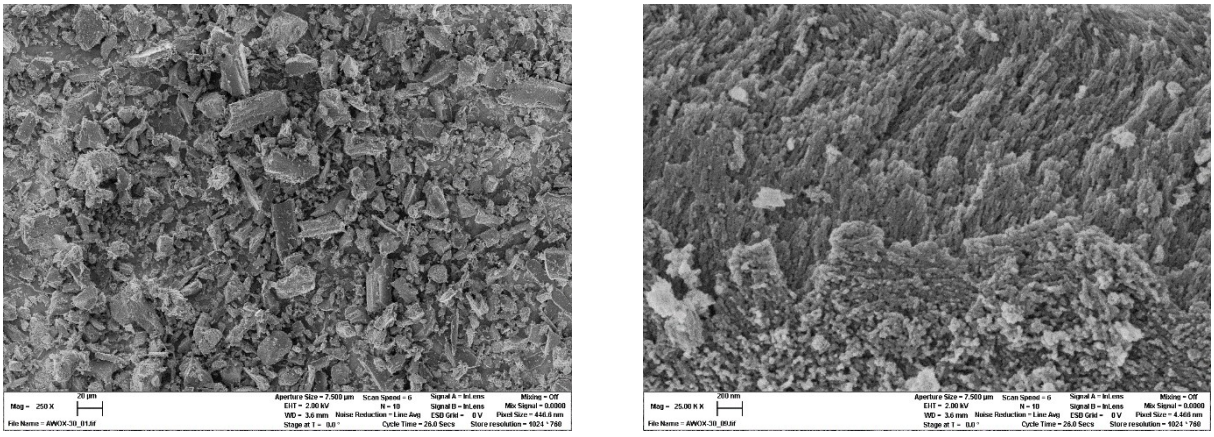

Figure S 20: SEM images of impregnated NCASPF at magnifications of 250x and 25,000x.

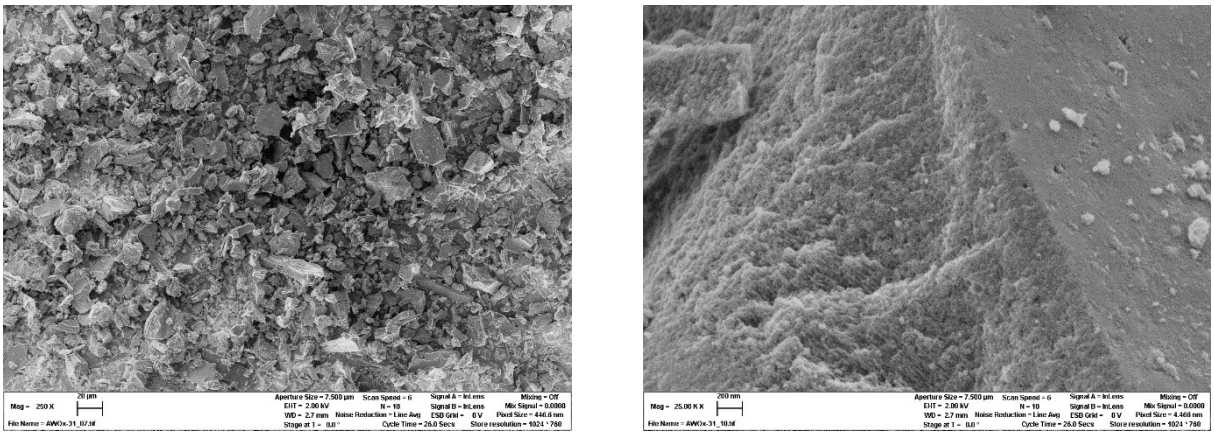

Figure S 21: SEM images of impregnated DKB-G at magnifications of 250x and 25,000x.

Supporting HPA-5 on CW20 by different synthesis methods

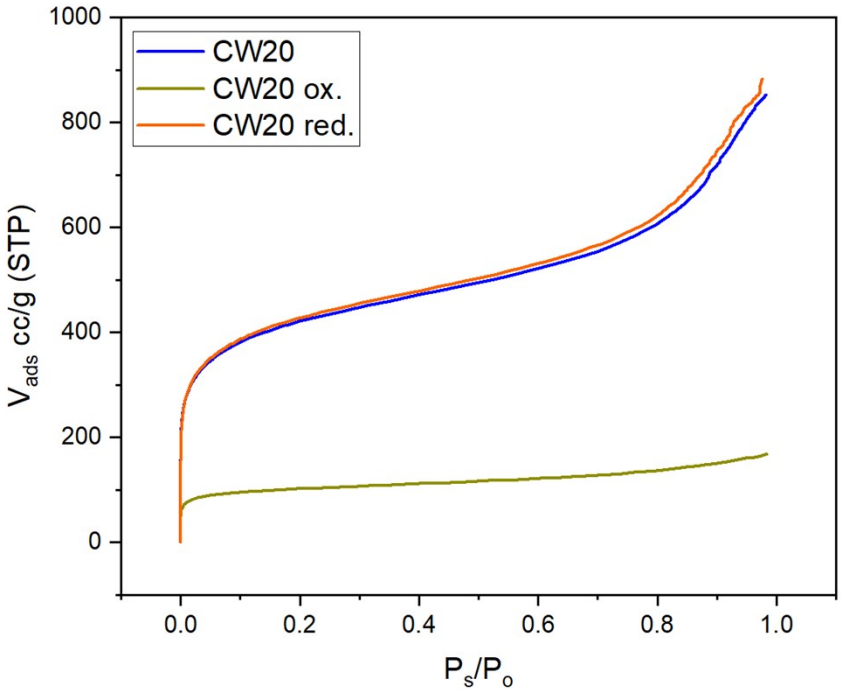

Figure S 22: Adsorption isotherms of untreated CW20 and pretreated $CW20_{ox.}$ and $CW20_{red.}$

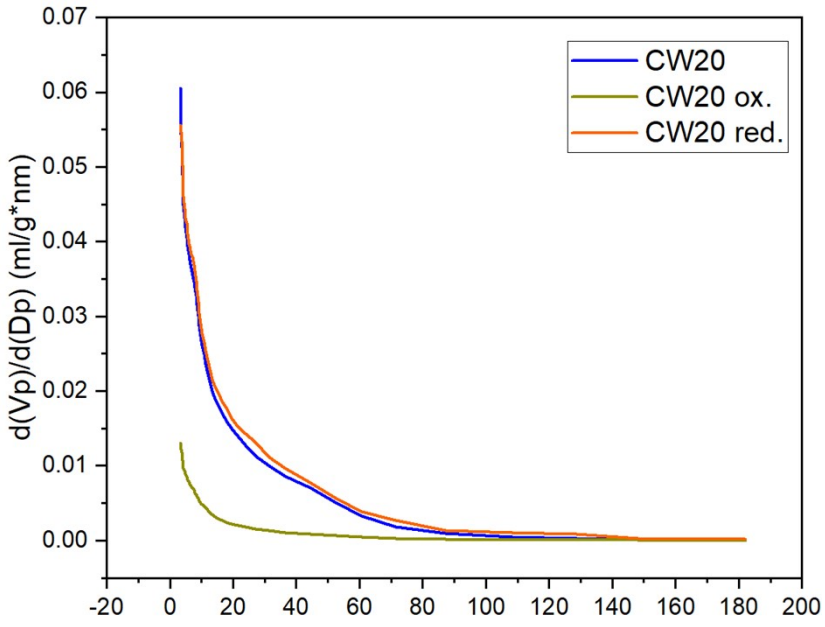

Figure S 23: Pore volumina of untreated CW20 and pretreated $CW20_{ox.}$ and $CW20_{red.}$

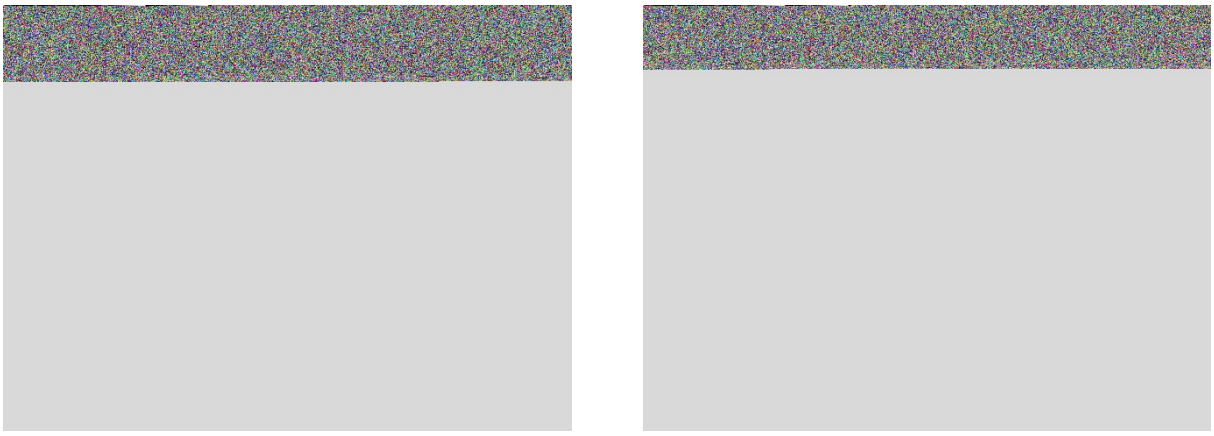

Figure S 24: SEM images of pure CW20 at magnifications of 250x and 25,000x.

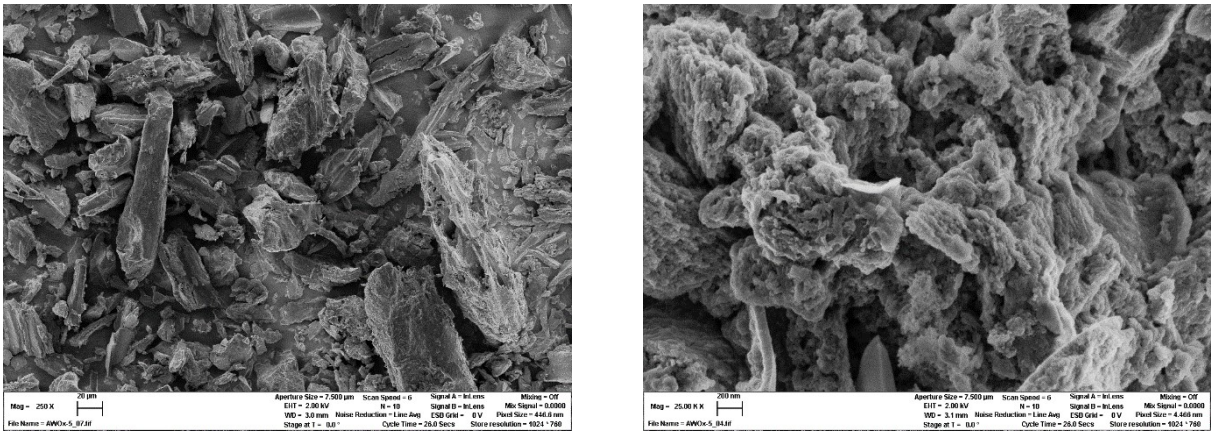

Figure S 25: SEM images of oxidized CW20 at magnifications of 250x and 25,000x.

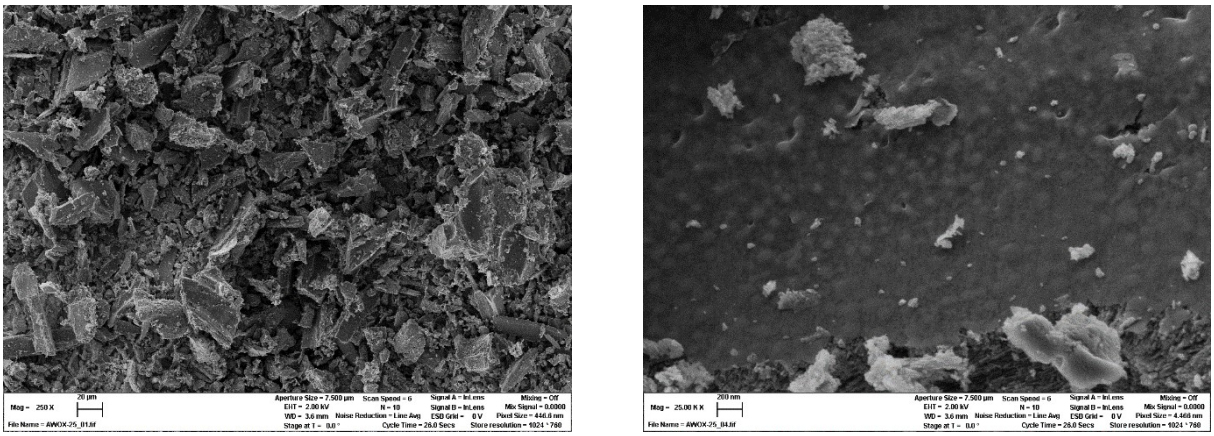

Figure S 26: SEM images of reduced CW20 at magnifications of 250x and 25,000x.

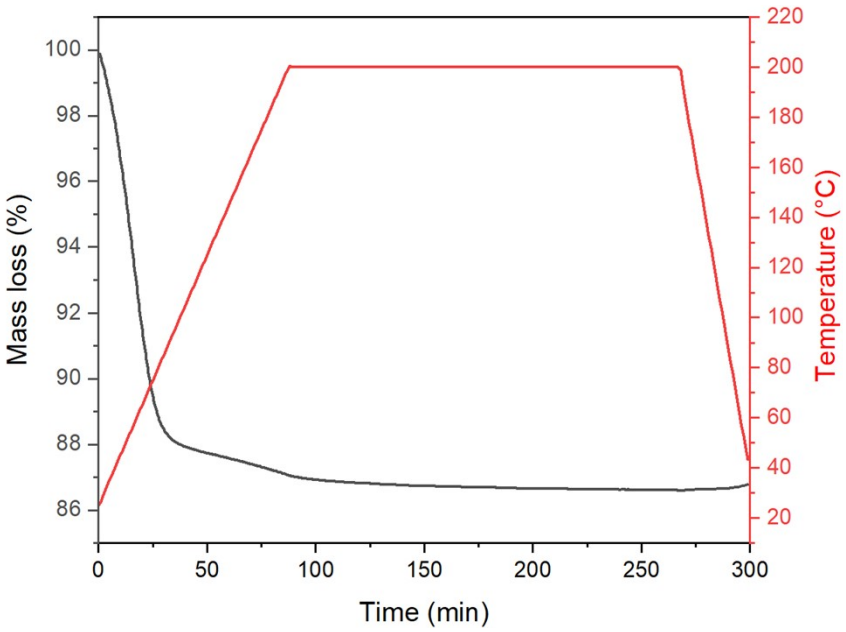

Figure S 27: TGA spectra of CW20 impregnated with HPA-5 (before washing).

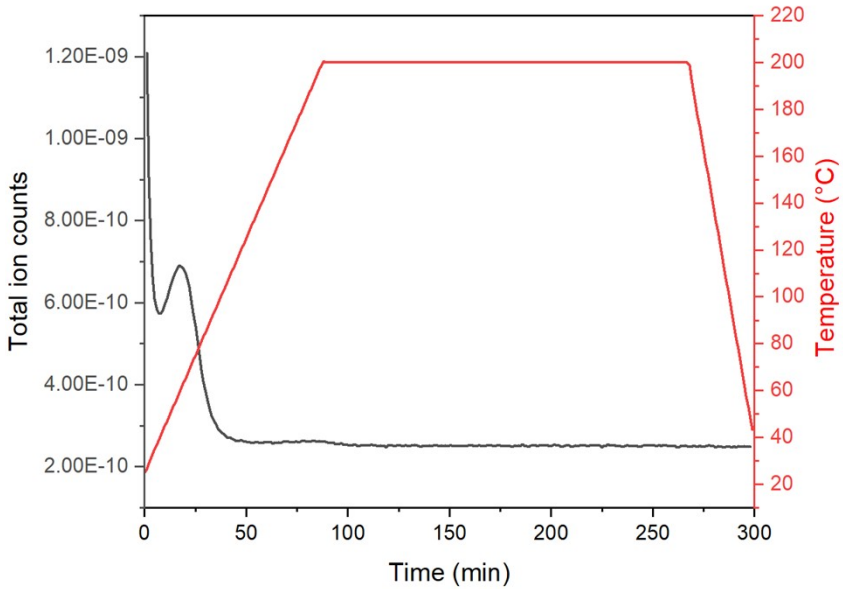

Figure S 28: Total ion counts (TIC) of TGA spectra of CW20 impregnated with HPA-5 (before washing).

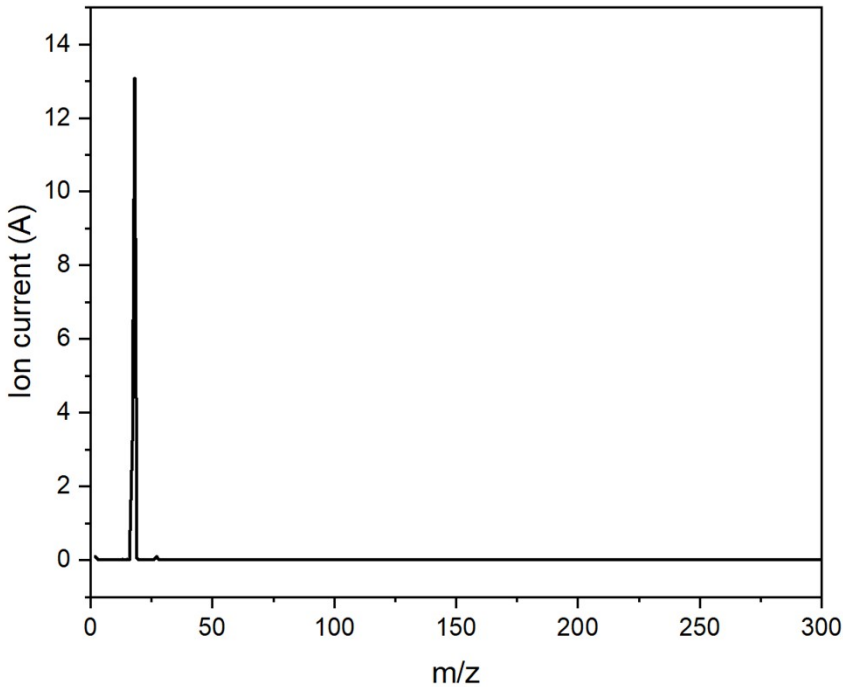

Figure S 29: m/z of maxima of maximum (TIC).

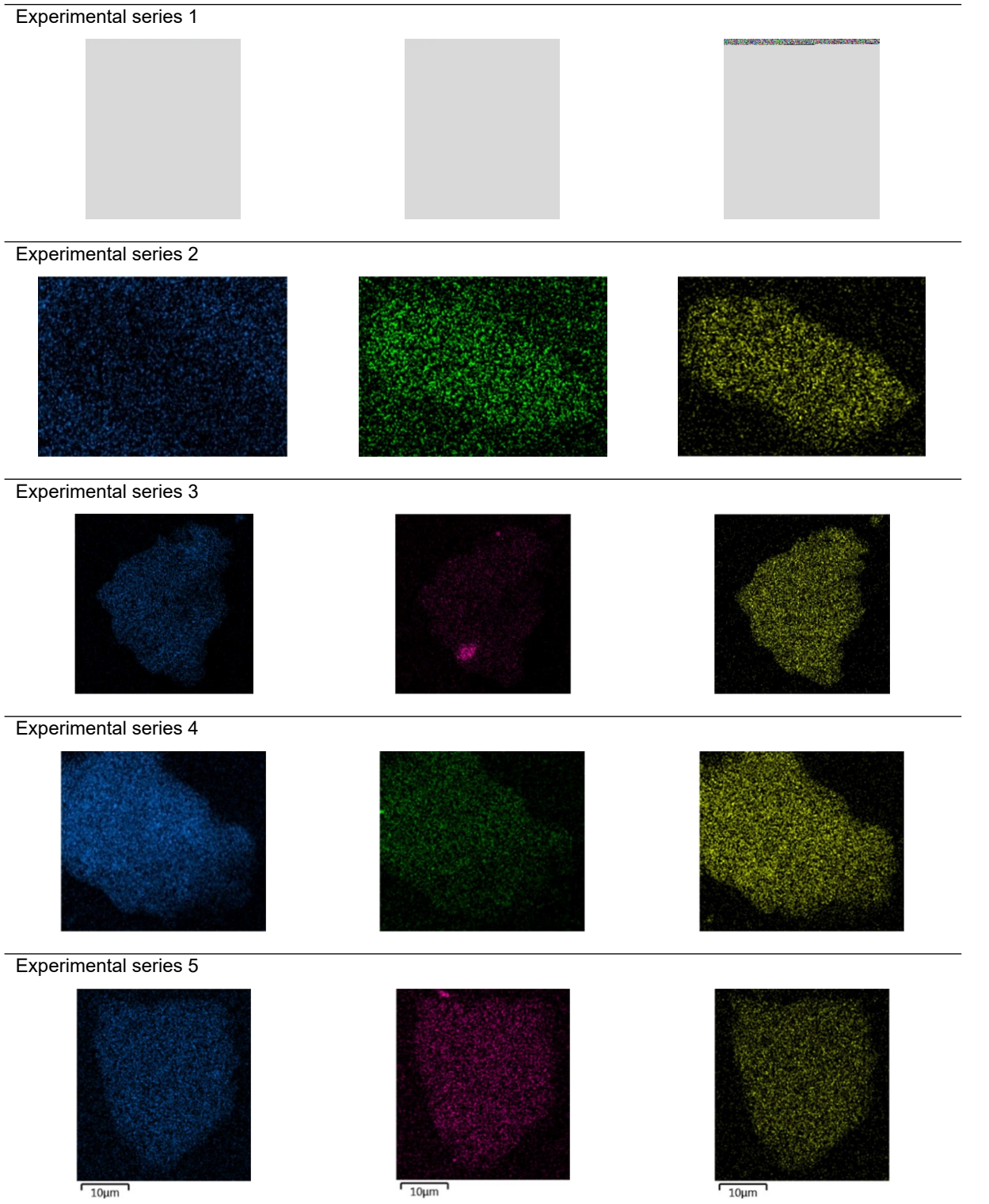

Figure S 30: SEM-EDX Mapping of CW20 after impregnation with different experimental series *with Mo (blue), P (green & pink) and V (yellow).*

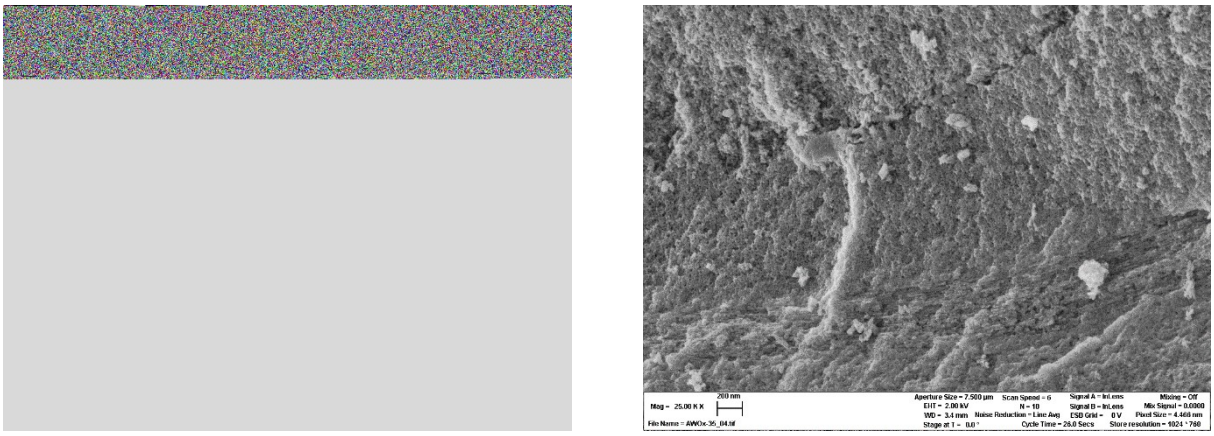

Figure S 31:SEM images of CW20_HPA-5 (exp. ser. 1) at magnifications of 250x and 25,000x.

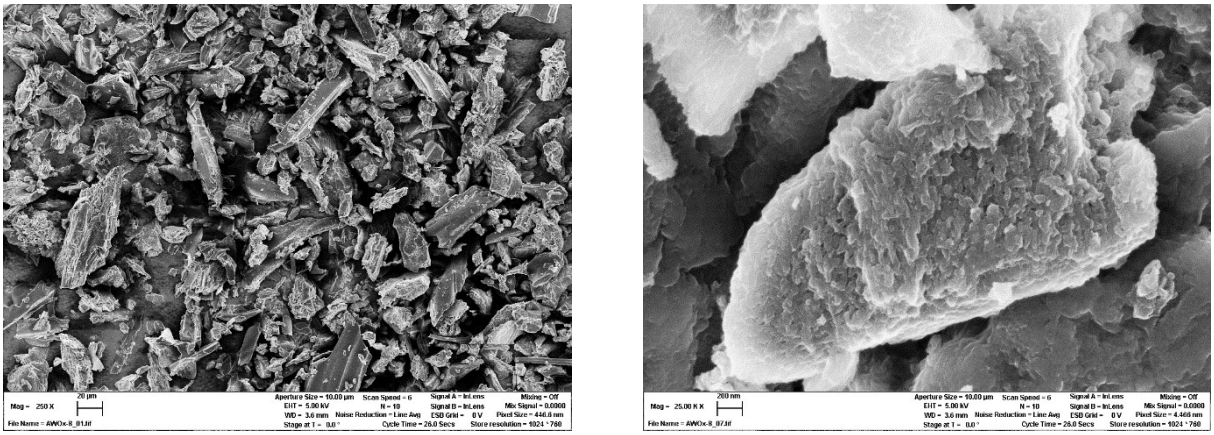

Figure S 32: SEM images of CW20_HPA-5 (exp. ser. 2) at magnifications of 250x and 25,000x.

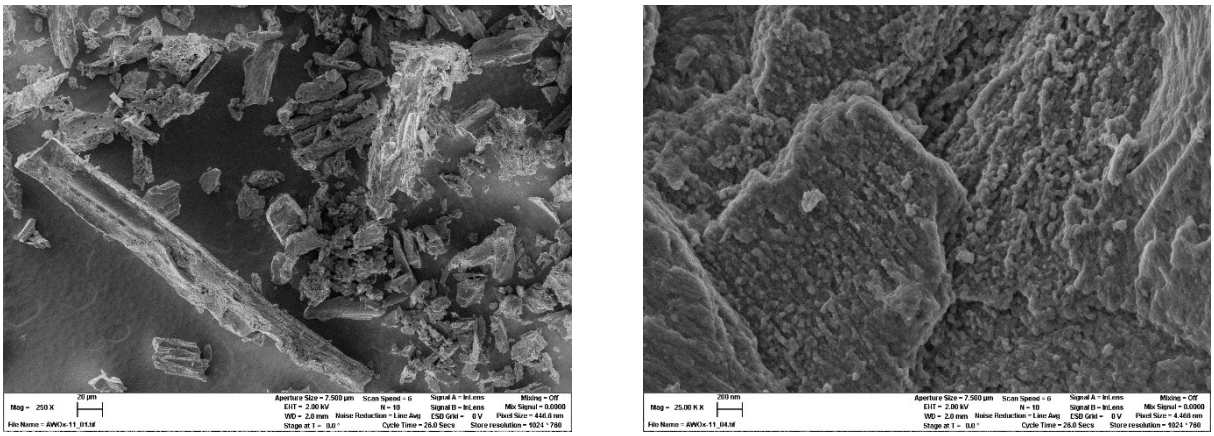

Figure S 33: SEM images of CW20_HPA-5 (exp. ser. 3) at magnifications of 250x and 25,000x.

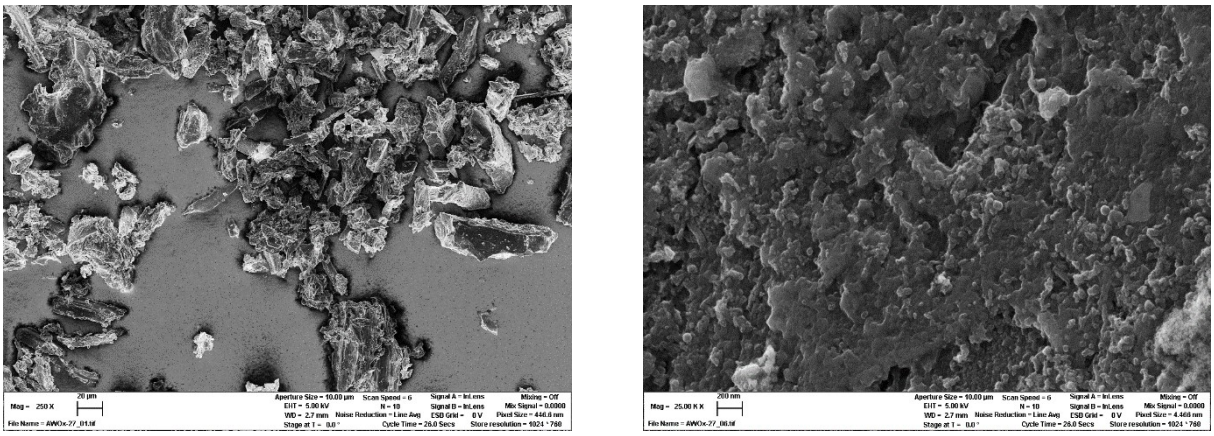

Figure S 34: SEM images of CW20_HPA-5 (exp. ser. 4) at magnifications of 250x and 25,000x.

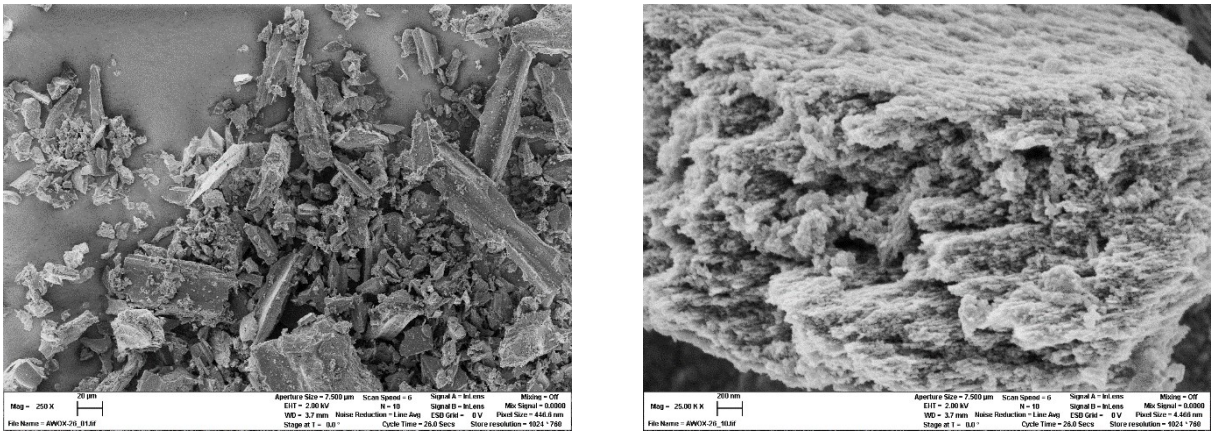

Figure S 35: SEM images of CW20_HPA-5 (exp. ser. 5) at magnifications of 250x and 25,000x.

Supplementary catalytic evaluation and determination of catalytic parameters

Catalytic experiments

The catalytic experiments were conducted in a three-fold plant consisting of three 100 mL stainless-steel (1.4571) reactor vessels made by HALMOSI. For stirring, a stainless-steel (1.4571) gas-entraining stirrer by Parr was used which was powered by an IKA Ministar 20. Graphite-based gaskets (Novaphit® MST/XP) were applied to provide reactor tightness. Each reactor was supplied with a heating jacket and two independent PT-100 thermostats measured the temperatures of the liquid phase inside the reactor and of the reactor wall. The pressure was measured both by analogous and digital pressure gages. Both temperature and pressure were regulated by Eurotherm controllers.

For the reaction, glass liners (21 mL tare volume) made of quartz glass fitting a maximum volume of 55 mL were utilized. For the oxidation, both glucose and catalyst were weighed and transferred to the glass liners – for glucose a mass of 3.603 g (20 mmol) and for the catalyst a mass of 1.821 g (pure HPA-5: 1.14 mmol). For the retro-aldol reaction, for glucose a mass of 1.032 g (5.7 mmol) and for the catalyst a mass of 0.406 g (pure HPA-5: 0.25 mmol)

Subsequently, the glass liner was filled with 45 mL (oxidation) or 40 ml (retro-aldol condensation) of deionized water. The glass liner was then transferred to the reactor vessel and the reactor was closed tightening five screws at a maximum torque of 15 Nm. To remove the air inside the reactor, three purges with O_2 were conducted. For the first two purges the pressure was elevated to 10 bar and for the last purge to 25 bar. The third purge at elevated pressure was also used to detect any leakages. The pressure was then set to 20 bar O_2 (oxidation) or N_2 (retro-aldol condensation), the stirrer was set to 300 rpm and the temperature was set to 90 °C (oxidation) or 160 °C (retro-aldol condensation). Once the temperature was reached, the stirrer was set to 1000 rpm, which was the reaction start point.

After 6 h (oxidation) or 1 h (retro-aldol condensation), the reaction was stopped by setting stirrers to 300 rpm, dismantling heating jackets and using pressurized air to cool down the reactors to 30 °C (approx. for 15 min). Gas samples were taken and the suspension inside the glass liners was filtered. Lastly, the filter cake was washed with 50 mL of water and dried for 24 h at 40 °C.

Analysis of substrates and reaction products

ICP-OES

Analogous to catalyst characterization

Infrared spectroscopy

Analogous to catalyst characterization

HPLC

The liquid reaction solution underwent quantitative analysis via High-Performance Liquid Chromatography (HPLC), employing a SHIMADZU HPLC system. This system was equipped with a BIORAD Aminex HPX-87H column (300 mm x 7.8 mm) and a refractive index detector for the analysis. For the conversion of glucose to formic acid, the HPLC analysis included an injection volume of 10 µL, a column temperature of 45 °C, and a flow rate of 0.5 ml/min. In the analysis of glucose conversion to lactic acid, the procedure involved an injection volume of 10 µL, a column temperature maintained at 30 °C, and a flow rate set at 0.3 ml/min.

HPLC determination of retention time and calibration for catalyst screening was performed using the following chemicals: glucose (n.a. Merck Milipore, 1.08337.1000), mannose (≥99 %, Sigma Aldrich, M2069-25G), fructose (≥99 %, VWR, 0226-1KG), glyoxal (40 %, Merck, 8206100100), glyceraldehyde (≥90 %, VWR, G5001-5G), erythrose, (75 %, Sigma Aldrich, E7625-1G), glycoaldehyde (), formic acid (99-100 %, AnalaR Normapur, 20318.322), acetic acid (79-81 %, Carl Roth, 20G164011), lactic acid (90 %, GPR Rectapur, 20356.298), acetaldehyde (≥99 %, VWR, 20877.265).

GC

Quantitative analysis of the gaseous reaction products was performed using a Varian 450-GC, which is equipped with column Shin Carbon ST (2 m · 0.75 mm) and with both a TCD-GC detector and an FID detector. The GC analysis protocol involved heating the system to 140°C at a rate of 15 K/min, followed by a holding period of 2.83 minutes. The TCD system operated with an argon flow at 300 °C, while the FID

was maintained at 200 °C, utilizing a hydrogen flow of 30 ml/min for combustion and an air flow of 310 mL/min.

Calculation of catalytic parameters

The conversion of glucose $X_{glucose}$ yield for all products (Y_P), the selectivities towards formic acid (S_{FA}) and lactic acid (S_{LA}), as well as the turnover-number (TON) were determined using the following equations:

$$X_{glucose} = \frac{n_{glucose,initial} - n_{glucose.\ final}}{n_{glucose.\ initial}} \cdot 100\ \% \quad \text{(S1)}$$

$$Y_P = \frac{n_p}{n_{glucose.\ initial}} \cdot 100\ \% \quad \text{(S2)}$$

$$S_{FA/LA} = \frac{Y_{FA/LA}}{X_{glucose}} \cdot 100\ \% \quad \text{(S3)}$$

Here, $n_{glucose,inital}$ represents the initial amount of glucose used, and $n_{glucose,final}$ denotes the amount of glucose remaining at the end of the reaction. N_p signifies the molar amount of specified product, n_{ps} encompasses the molar amounts of all resulting products.

Supplementary catalytic results and characterization

Applying supported HPA-5 for the catalytic conversion of glucose

Oxidative conversion of glucose analogous to the OxFA process

Table S 4: Catalytic parameters for conversion of glucose to formic acid.

	1	2	3	4	5	blank	HPA-5
	Yields (%)						
Fructose	1.13	0.49	1.57	1.57	1.49	1.22	1.07
Glyoxal	1.35	6.44	2.47	2.47	1.87	0.00	3.21
Glycerinaldehyde	6.08	2.02	5.73	5.72	7.30	0.00	5.34
Erythrose	7.50	3.60	7.64	7.63	8.39	0.00	0.00
Glycoaldehyde	1.80	2.62	3.82	3.82	1.95	0.00	0.00
Formic Acid	31.11	24.13	34.43	34.38	31.86	0.00	40.49
Acetic Acid	0.30	0.15	1.27	1.27	0.37	0.00	0.53
Carbon dioxide	19.07	7.56	6.69	5.31	0.01	0.30	7.37
Carbon monooxide	1.54	1.04	0.46	0.14	0.00	0.00	0.30
Selectivity to formic acid (%)	39.92	44.57	50.41	48.86	45.37	0.00	53.43
Conversion (%)	77.94	54.14	68.30	70.36	70.23	2.38	75.78
Carbon balance	91.94	93.92	95.80	91.96	83.02	99.13	85.15
Initial pH	2.59	2.64	2.86	2.56	2.64	3.84	1.25
Final pH	1.38	1.32	1.03	1.30	1.28	2.69	1.39

Table S 5: Catalytic parameters for conversion of glucose to formic acid: Experimental series 1 (1) and repetition (1_rep.).

	1	1_rep.
	Yields	
Fructose	1.13	1.35
Glyoxal	1.35	2.32
Glycerinaldehyde	6.08	6.63
Erythrose	7.50	4.80
Glycoaldehyde	1.80	1.80
Formic Acid	31.11	27.43
Acetic Acid	0.30	0.00
Carbon dioxide	19.07	12.32
Carbon monooxide	1.54	3.00
Selectivity to formic acid	39.92	37.56
Conversion	77.94	73.02
Carbon balance	91.94	84.44

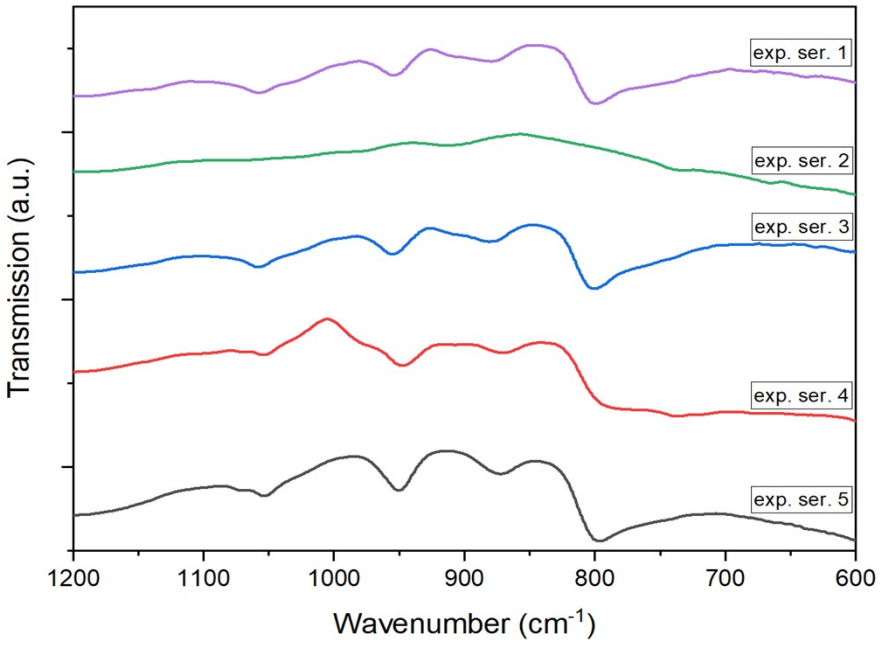

Figure S 36: IR-spectra of CW20 after impregnation with different experimental series after reaction (glucose to formic acid).

Inert conversion of glucose analogous to retro-aldol-condensation

Table S 6: Catalytic parameters for conversion of glucose to lactic acid.

	1	2	3	4	5	blank	HPA-5
	Yields (%)						
Mannose	29.79	24.69	32.75	32.65	25.19	4.34	29.74
Glyceraldehyde	0.45	0.58	0.34	0.40	3.54	0.00	0.45
Lactic Acid	10.32	8.44	9.76	9.82	6.07	0.00	10.30
Formic Acid	2.71	1.96	1.67	1.85	2.09	0.00	2.71
Acetic Acid	0.86	0.00	0.00	0.00	0.00	0.00	0.86
Acetaldehyde	3.09	1.78	4.09	4.58	1.88	0.00	3.09
CO_2	1.58	1.36	0.61	0.80	0.63	0.09	0.42
Selectivity to lactic acid (%)	14.55	13.00	14.88	14.98	9.22	0.00	14.51
Conversion	70.92	64.92	65.58	65.56	65.88	2.54	70.97
Carbon balance	77.90	73.89	83.64	84.55	73.52	100	76.59
Initial pH	2.96	3.16	2.93	2.97	3.40	5.77	1.92
Final pH	2.41	2.65	2.52	2.56	2.65	3.31	2.32

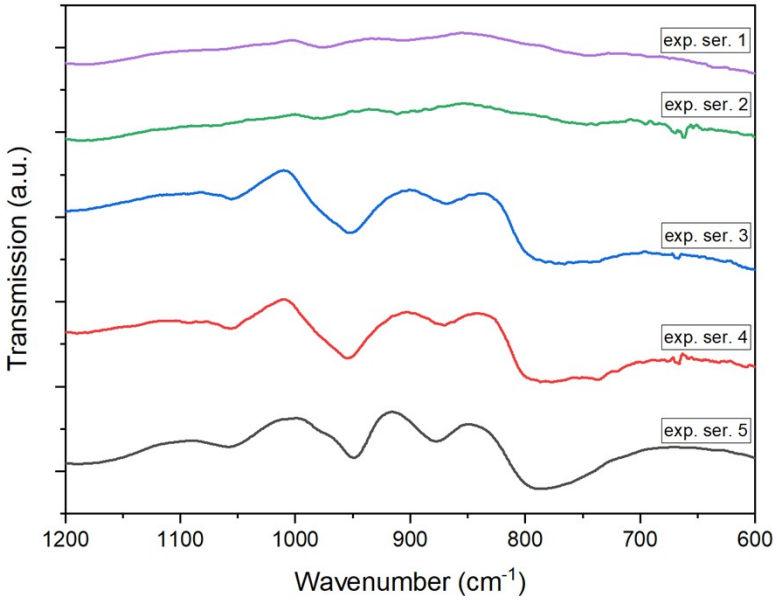

Figure S 37: IR-spectra of CW20 after impregnation with different experimental series after reaction (glucose to formic acid).

References

(1) Bandosz, T. J.; Jagiello, J.; Schwarz, J. A. Comparison of methods to assess surface acidic groups on activated carbons. *Anal. Chem.* **1992**, *64*, 891–895.

(2) Kohl, S. *Oberflächenoxide auf kohlenstoffbasierten Materialien.*, 2010.

(3) Fanning, P. E.; Vannice, M. A DRIFTS study of the formation of surface groups on carbon by oxidation. *Carbon* **1993**, *31*, 721–730.